Inferring Plasma Flows in the Solar Photosphere & Chromosphere using Deep Learning and Surface Observations

Benoit Tremblay[1,2,3], Kevin Reardon[3], Raphaël Attié[4,5], Maria D. Kazachenko[1,2,3], Andrés Asensio Ramos[6], Dennis Tilipman[2]

[1]Laboratory for Atmospheric & Space Physics, USA - [2]CU Boulder, USA - [3]National Solar Observatory, USA - [4]NASA Goddard Space Flight Center, USA - [5]George Mason University, USA - [6]Instituto de Astrofísica de Canarias, Spain

Abstract

Direct measurements of plasma motions are limited to the line-of-sight component at the Sun's surface. Multiple tracking and inversion methods were developed to infer the transverse motions from observational data. Recently, the fully convolutional DeepVel & DeepVelU neural networks were trained in conjunction with detailed magnetohydrodynamics (MHD) simulations of the Quiet Sun and sunspots to recover the instantaneous depth/height-dependent transverse velocity vector from a combination of intensitygrams, magnetograms and/or Dopplergrams of the solar surface. Through this supervised learning approach, the neural network attempts to emulate the synthetic flows, and by extension the physics, from the numerical simulation it was presented during its training, i.e. its outputs are model-dependent and may be subjected to biases. Although simulations have become increasingly realistic, the validity of flows inferred by DeepVel or DeepVelU is subject to debate when using real observational data as input. As a test, we use white light images of the Quiet Sun photosphere (optical depth tau=1) produced by the Interferometric BIdimensional Spectropolarimeter (IBIS) installed at the Dunn Solar Telescope to infer plasma motions approx. 150-200 km above the surface (i.e., near the transition between the photosphere and the chromosphere) using DeepVel. We discuss work in progress comparing the neural network estimates to the optical flows determined from a time series of observational data formed near 150-200 km above the surface. Optical flows do not directly track actual transverse plasma motions, but are correlated with physical flows over certain spatial and temporal scales.

1. Introduction: Transverse Plasma Flows on the Sun

From spectropolarimetric inversions of the Sun, we can estimate the line-of-sight component of surface plasma velocities. Multiple tracking and inversion methods were developed to infer transverse velocities from observational data. Recently, neural networks were trained in conjunction with magnetohydrodynamics simulations of the photosphere+atmosphere to recover the depth/height-dependent transverse velocity vector from solar surface data [1,7,8,9].

Q: Are transverse flows inferred through supervised deep learning realistic ?

We propose the following tests: Using the DeepVel neural network [1], we

- reconstruct transverse velocities at the solar surface ($\tau \approx 1$),
- extrapolate transverse velocities above the surface ($z \approx$ 150-200 km)

from surface observations captured by the Interferometric BIdimensional Spectropolarimeter (IBIS) installed at the Dunn Solar Telescope (DST), and we compare inferred flows to large scale optical flows computed by FLCT [3] and Balltracking [2; not shown in this poster] from

- IBIS 7200Å images ($\tau \approx 1$) with Δt=12 s and Δx=70 km,
- IBIS 7090Å images ($z \approx$ 150-200 km above the surface) with Δt=12 s and Δx=70 km.

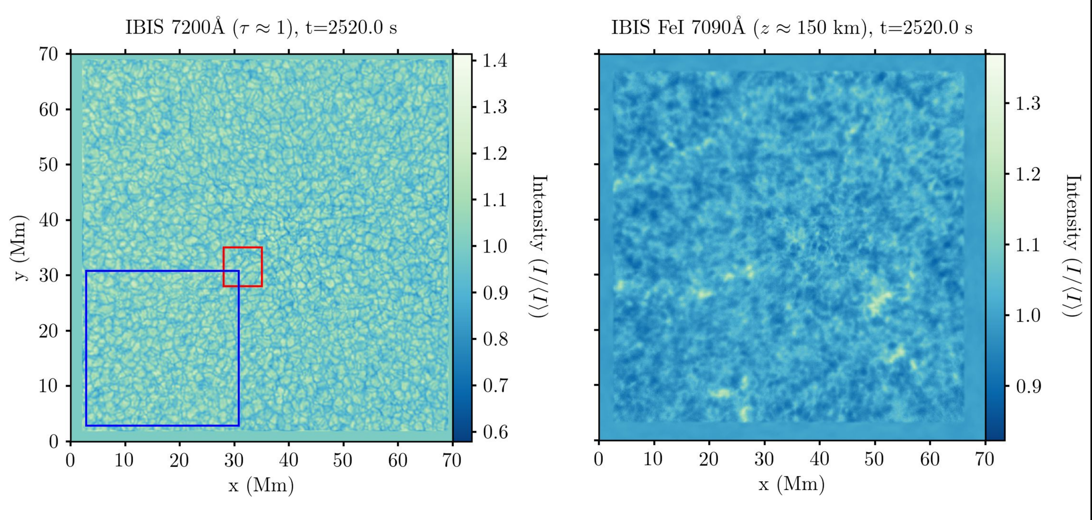

Figure 1: IBIS data at 7200Å (surface) and 7090Å (≈150-200 km above the surface).

2. DeepVel Neural Network

DeepVel[1] is a convolutional neural network trained using numerical simulations to map transverse flows at optical(τ)/geometrical(z) heights from surface data.

We trained different versions of **DeepVel** using:

- **STAGGER** [7]: Δt=60 s, Δx=96 km;
  - Infer $\vec{v}_t(\tau \approx 1, t_i)$ from $I_c(\tau \approx 1, t_{i,i+1})$.
- **MURaM** [10]: Δt=2 s, Δx=16 km;
  - Infer $\vec{v}_t(\tau \approx 1, t_i)$ from $I_c(\tau \approx 1, t_{i,i+1})$.
  - Infer $\vec{v}_t(z \approx 160\ \mathrm{km}, t_i)$ from $I_c(\tau \approx 1, t_{i,i+1})$.

Data preparation steps performed:

- Convolution with the DST theoretical PSF.
- Downsampling to Δx=70 km (IBIS pixel size).
- Training set: Random patches & augmentation.

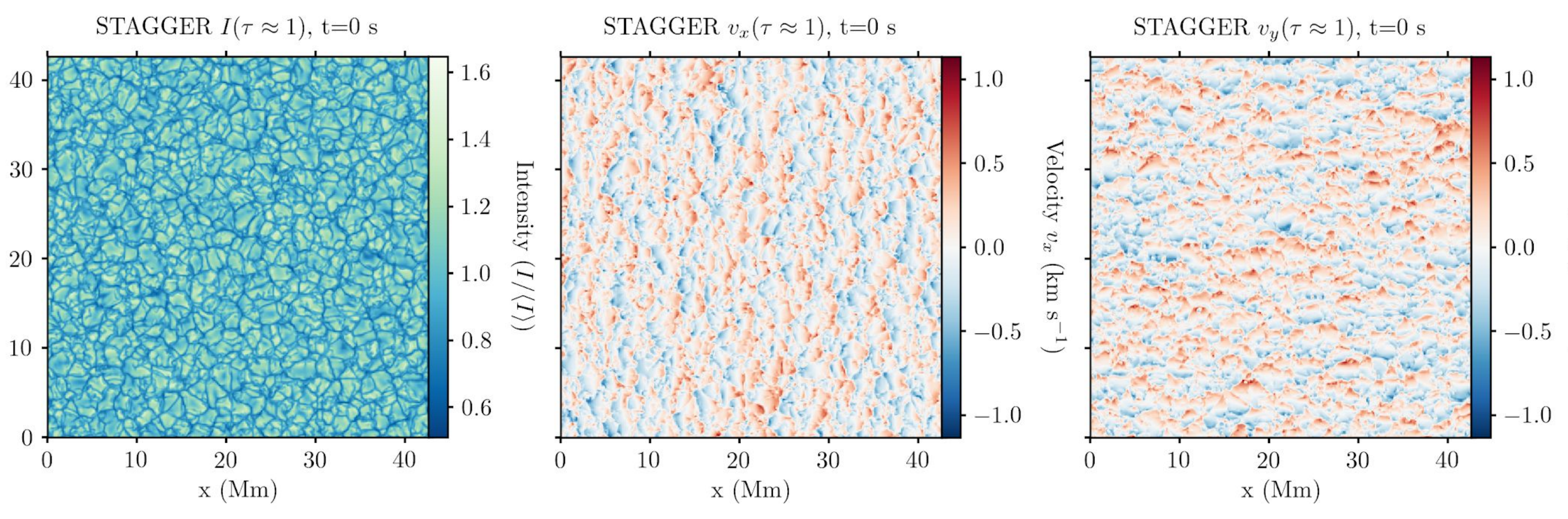

Figure 2: Examples of slices at $\tau \approx 1$ from the STAGGER simulation that were used to train the DeepVel neural network.

3. Reconstruction of Transverse Velocities at the Surface from Simulation Data and IBIS Observations

We test against STAGGER data a version of DeepVel that was trained using the STAGGER dataset.

Figure 3: Transverse velocities computed at $\tau \approx 1$:
(a) by the STAGGER simulation $\vec{v}_{\mathrm{ref}}$ (reference),
(b) by DeepVel $\vec{v}_{\mathrm{D}}$ (reconstruction).
The surface intensity $I_c(\tau \approx 1)$ is displayed as colored background for context. Metrics Eabs, C, A measure the abs. errors $\mathrm{E_{abs}}(\vec{v}_{\mathrm{ref},t}, \vec{v}_{\mathrm{D},t}) = \left\langle \sqrt{(\vec{v}_{\mathrm{ref},t} - \vec{v}_{\mathrm{D},t}) \cdot (\vec{v}_{\mathrm{ref},t} - \vec{v}_{\mathrm{D},t})} \right\rangle$,
correlation coef. $\mathrm{C}(\vec{v}_{\mathrm{ref}}, \vec{v}_{\mathrm{D},t}) = \dfrac{\langle \vec{v}_{\mathrm{ref},t} \cdot \vec{v}_{\mathrm{D},t} \rangle}{\sqrt{\langle \vec{v}_{\mathrm{ref},t} \cdot \vec{v}_{\mathrm{ref},t} \rangle \langle \vec{v}_{\mathrm{D},t} \cdot \vec{v}_{\mathrm{D},t} \rangle}}$,
normalized dot product $\mathrm{A}(\vec{v}_{\mathrm{ref},t}, \vec{v}_{\mathrm{D},t}) \equiv \left\langle \dfrac{\vec{v}_{\mathrm{ref},t} \cdot \vec{v}_{\mathrm{D},t}}{\|\vec{v}_{\mathrm{ref},t}\| \, \|\vec{v}_{\mathrm{D},t}\|} \right\rangle$.
Expected values are 0, 1 & 1 respectively. (c) Scatterplot comparing inferred and reference velocity components.

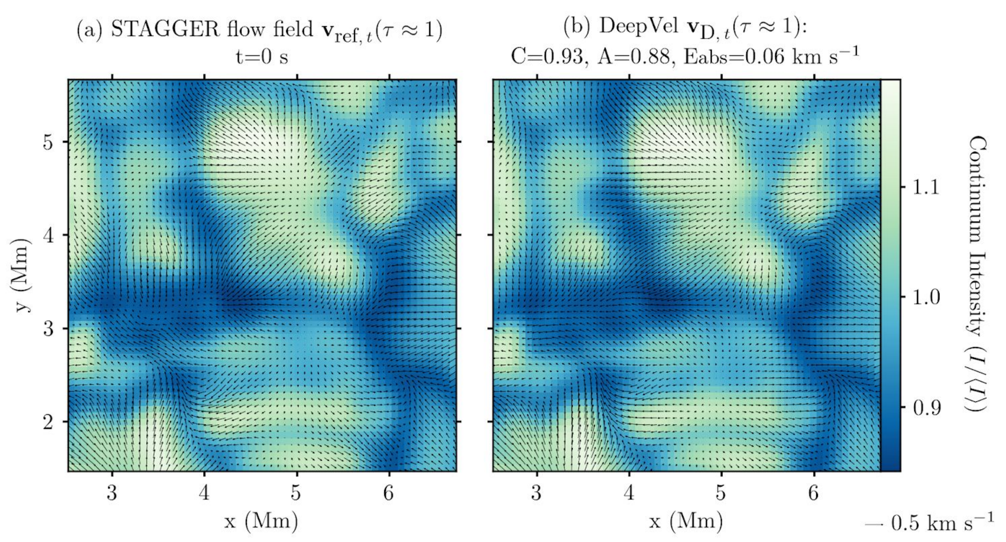

We test against MURaM data a version of DeepVel that was trained using the MURaM dataset.

Figure 4: Transverse velocities computed at $\tau \approx 1$:
(a) by the MURaM simulation $\vec{v}_{\mathrm{ref}}$ (reference),
(b) by DeepVel $\vec{v}_{\mathrm{D}}$ (reconstruction).
The vertical velocity $v_z(\tau \approx 1)$ is displayed as colored background for context. Metrics Eabs, C, and A measure the mean absolute errors, correlation coefficient, and normalized dot product between flow fields, with expected values of 0, 1 and 1 respectively. (c) Scatterplot comparing inferred and reference velocity components. Notice the difference in flow amplitudes between MURaM and STAGGER (Figure 3).

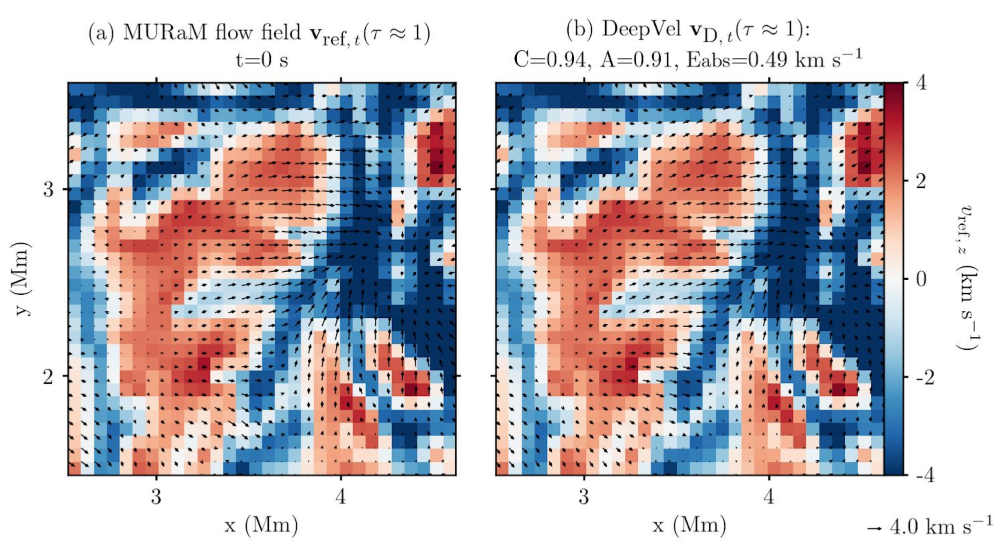

We test against MURaM data a version of DeepVel that was trained using the STAGGER dataset.

Figure 5: Transverse velocities computed at $\tau \approx 1$:
(a) by the MURaM simulation $\vec{v}_{\mathrm{ref}}$ (reference),
(b) by DeepVel $\vec{v}_{\mathrm{D}}$ (reconstruction).
The vertical velocity $v_z(\tau \approx 1)$ is displayed as colored background for context. Metrics A and C suggest a good agreement in terms of the flow structures generated, but absolute errors are significantly larger than for Figure 4. (c) Inferred transverse velocities are more scattered about the black line than fore Figure 4(c). These results illustrate the model-dependency of DeepVel.

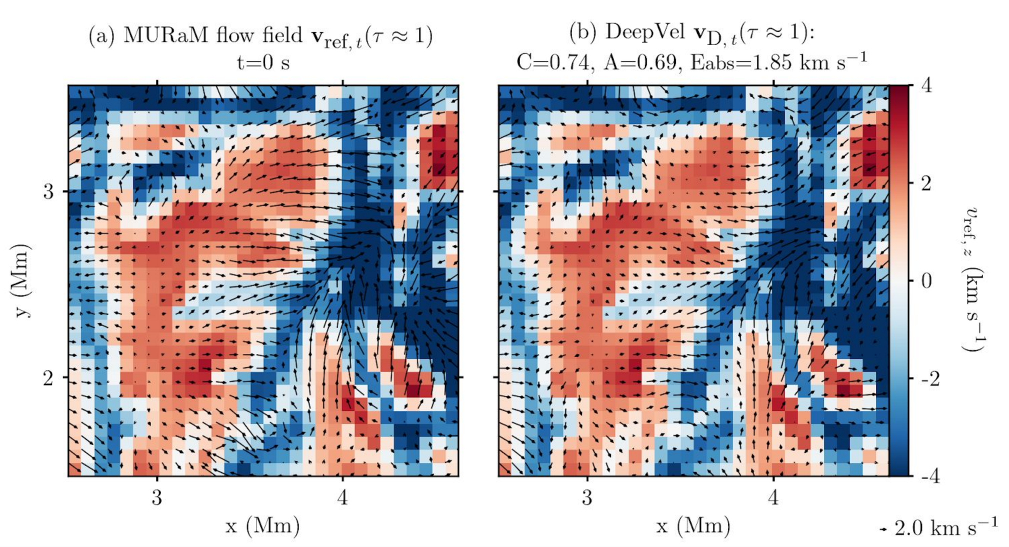

We compare the large scale surface flows inferred by DeepVel from IBIS 7200Å images to optical flows computed from IBIS 7200Å images.

Figure 6: Transverse velocities computed at $\tau \approx 1$:
(a) by Fourier Local Correlation Tracking [FLCT: 3],
(b) by DeepVel trained using STAGGER data (Figure 3),
(c) by DeepVel trained using MURaM data (Figure 4).

A 28 Mm by 28 Mm subfield from 30-minute averaged IBIS 7200Å images (blue rectangle in Figure 1) is displayed as colored background for context. DeepVel flows were averaged over 30 minutes and then smoothed using a boxcar filter with FWHM=2.5 Mm to maximize the correlation between optical flows (e.g., FLCT) and physical flows. Note the difference in arrow length between the two versions of DeepVel due to the different training simulation properties.

Scatterplots differ in terms of slope when comparing FLCT optical flow components to the transverse velocities inferred by DeepVel (d) trained using the STAGGER dataset and (e) trained using the MURaM dataset. There is no ground truth, hence we cannot determine what amplitudes are most realistic. DeepVel inferences were performed using training simulation properties (i.e., the mean and the standard deviation of the simulation flows) and could be adjusted with a linear correction.

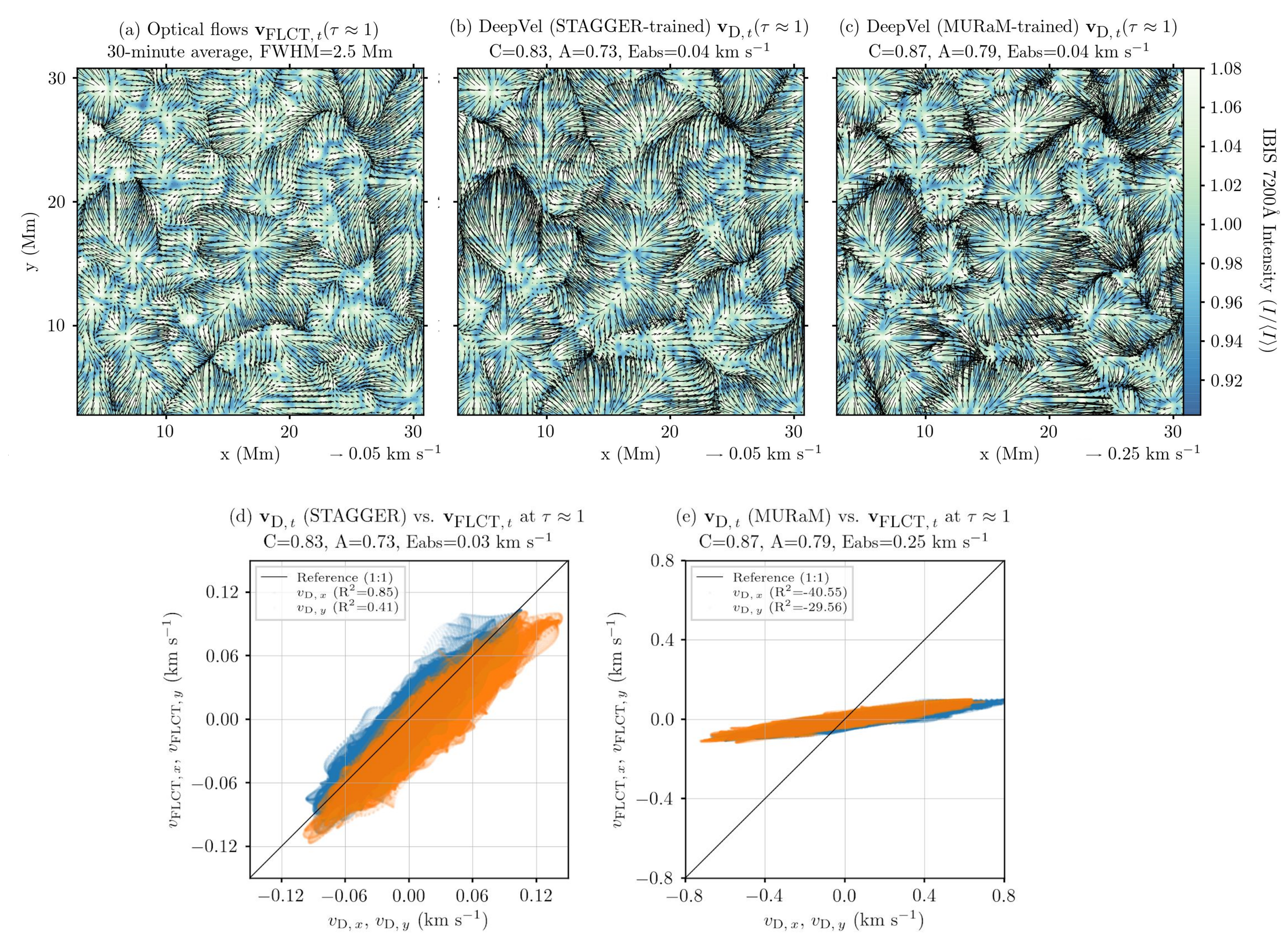

We look at the small scale surface flows inferred by DeepVel from IBIS 7200Å images.

Figure 7: (a) IBIS 7200Å image of the surface of the Sun (field of view of 70 Mm by 70 Mm). (b) Velocity field inferred by DeepVel (i.e., the version from Figure 3) within a subfield identified by a red rectangle in the IBIS image. Like in the simulations, flows are divergent inside granules and convergent inside intergranular lanes. No comparison with optical flows is performed at small scales as optical flows become more and more decorrelated from physical flows at subgranular scales.

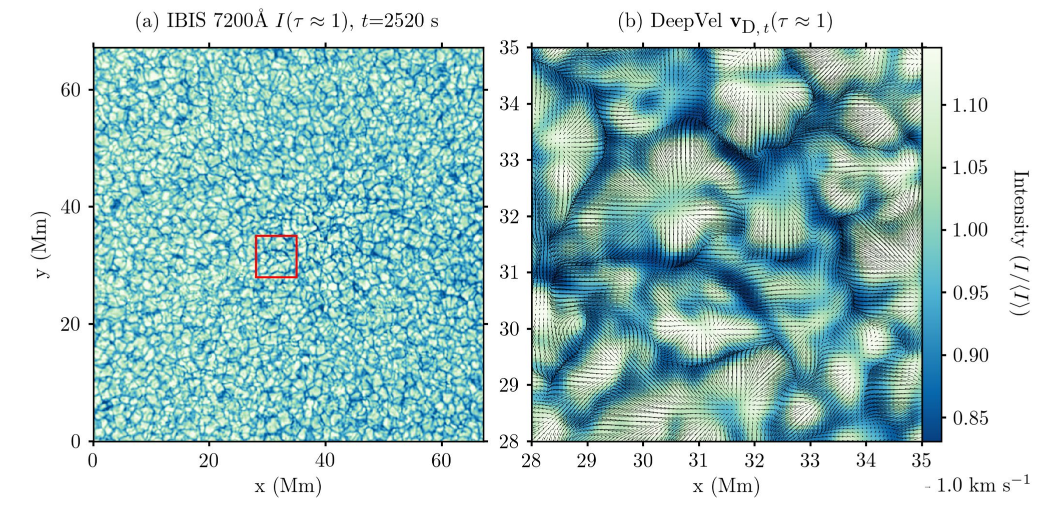

(Click image for video version)

4. Work in Progress: Extrapolation of Transverse Velocities Above the Surface from Simulation Data and IBIS Observations

We test against MURaM data a version of DeepVel that was trained using the MURaM dataset.

Figure 8: Transverse velocities computed at $z \approx 160$ km:
(a) by the MURaM simulation $\vec{v}_{\mathrm{ref}}$ (reference),
(b) by DeepVel $\vec{v}_{\mathrm{D}}$ (reconstruction).
The vertical velocity $v_z(z \approx 160\ \mathrm{km})$ is displayed as colored background for context. Metrics Eabs, C, and A measure the mean absolute errors, correlation coefficient, and normalized dot product between flow fields, with expected values of 0, 1 and 1 respectively. (c) Scatterplot comparing inferred and reference velocity components. **Despite being extrapolations from surface data, flow field inferences by DeepVel perform quite well.**

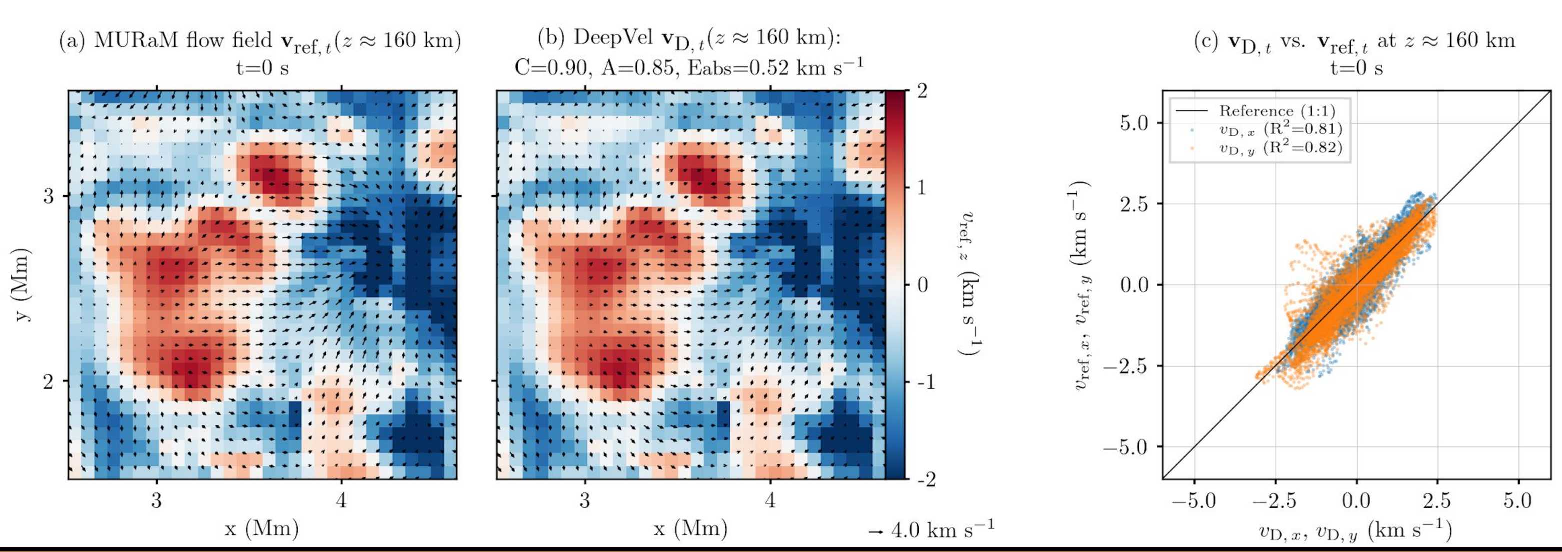

We look at the small scale flows extrapolated above the surface by DeepVel from IBIS 7200Å images.

Figure 9: (a) IBIS 7090Å image from 150-200 km above the solar surface. (b) Velocity field extrapolated at z=160 km by DeepVel (i.e., the version from Figure 7) within a subfield identified by a red rectangle in the IBIS image.

Comparisons between large scale flows extrapolated from 7200Å images and optical flows computed from 7090Å images are left as future work as the height of formation of the 7090Å images needs to be better constrained.

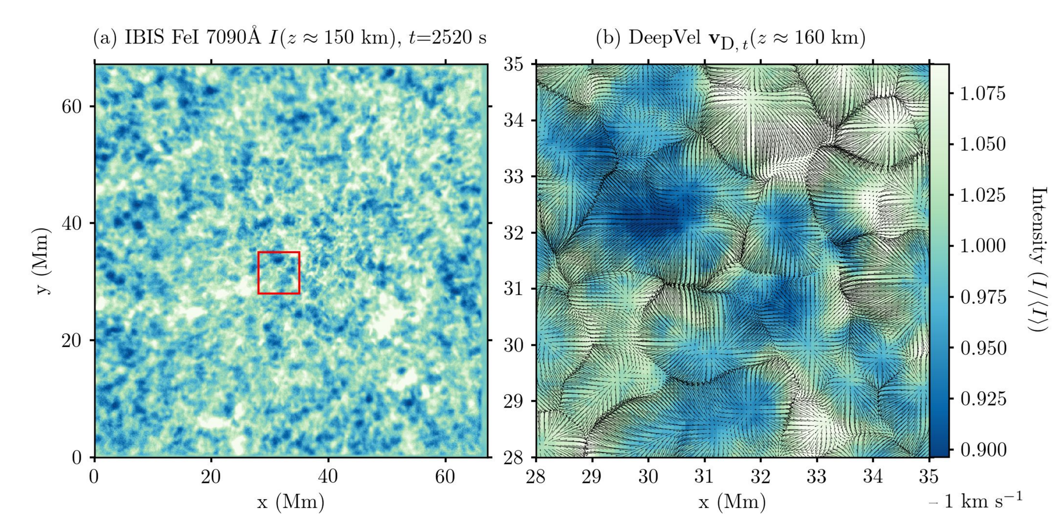

(Click image for video version)

5. Conclusions & Future Work

In conclusion:

- Surface: Large-scale flows generated by DeepVel form structures similar to optical flows, but differ in amplitude depending on the model used for training.
- Surface: Small-scale flows generated by DeepVel are consistent with simulations.
- Above the surface: Tests performed with simulation data suggest that DeepVel can extrapolate flows above the surface.

Future work:

- Data preparation: Account for stray light.
- Above the surface: Identify more precisely the height of formation of IBIS 7090Å data, retrain DeepVel, and perform comparison with optical flows.
- Large scale flows: Compare with optical flows computed using Balltracking [2; not shown in this poster, but large-scale surface flows form structures similar to FLCT].

References

[1] Asensio Ramos et al., 2017
[2] Attié et al., 2018
[3] Fisher & Welsch, 2008
[4] Kazachenko et al., 2014
[5] Schrijver et al., 2006
[6] Stein & Nordlund, 2012
[7] Tremblay et al., 2021
[8] Tremblay & Attié, 2020
[9] Tremblay et al., 2018
[10] Vögler et al., 2005

Recording

Click here to watch a recording of a seminar that was presented at the National Solar Observatory in February 2021.